Thermal Cycles in Multiple Electrode Submerged Arc Welding

The interrelationship of thermal cycles, bead shape and welding parameters is characterized

BY N. U. AHMED AND B. L. JARVIS

ABSTRACT. Multiple electrode submerged arc welding (SAW) is often used to increase the deposition rate in high productivity fabrication. However, while the development and application of the process have succeeded, the approach has not been systematic, and there is limited scientific information available regarding the process. This paper is concerned with the thermal cycles and resulting weld bead shape in four-electrode SAW. The experimental data were obtained with embedded thermocouples, by macroscopic examination of sections, and by weld pool ejection. The discussion considers the relationships between the welding conditions, the thermal responses and bead profiles. Data describing the geometry of the solidification boundary during the welding process are included and used to augment the description of the heat flow outside the weld pool. The study concludes that one may anticipate and control many features of the thermal response and bead profile.

Introduction

Multiple electrode submerged arc welding (SAW) has been gaining in popularity since being described in the early '50s (Ref. 1), due to its potential for high weld metal deposition rates. Currently, the process uses from two to ten electrodes (Ref. 2) to fabricate various elements in line pipes, ship structures and building structures. The use of higher than usual welding parameters (that is, values for current, voltage and speed) allows the deposition of more filler material at a particular heat input (per unit length) than is possible with other processes. These parameters, together with electrode size, spacing, inclination and electrical configuration, all influence the resulting weld properties.

It has been recognized that there is a need to study the thermal cycles in the multiple electrode process for predictive purposes (Ref. 3). In addition, limited x-ray fluoroscopy investigations (Refs. 4, 5) of weld pool formation, and the occurrence of discontinuities, have been reported. However, to our knowledge, the majority of thermal effects evaluated in SAW have dealt with single electrodes, and no detailed study during multiple electrode welding has been made. Thermal effects become more complicated in multiple electrode SAW due to the multiple arc-weld pool interactions, the influence of cooling rate, and the effect of current, voltage and speed on weldment characteristics. Moreover, since computer simulation techniques are becoming more popular with the fabrication industries, the question whether multiple electrode welding follows the same trends as single electrode welding, or behaves significantly differently, needs to be resolved.

KEY WORDS

SAW
Multiple Electrodes
Thermal Cycles
Peak Temperatures
Penetration
Arc Current
Voltage
Welding Speed
Heat Input
Weld Pool Ejection

The objective of this study was to make a qualitative examination of the characteristics of the HAZ thermal cycles generated in four-electrode submerged arc welding of steel plate. Since the detailed behavior within the pool is not yet well understood, it was considered legitimate to choose experimental conditions that were relatively simple, rather than those appropriate to a particular welding application. The main approach was temperature measurement using embedded thermocouples, but the examination of cross-sections, and of the craters left after weld pool ejection, were also employed. The data from these techniques were shown to be consistent with the formation of four overlapping weld pools. However, although the amount of overlap was often considerable, the cumulative effects on the peak temperature and penetration were less than anticipated, and as a result, a variety of unexpected behaviors was observed.

Experimental

Materials

Commercially available C-Mn steel plates of 20- and 50-mm (0.8- and 1.9-in.) thicknesses were used throughout this investigation. Each test piece was 500 mm long by 300 mm wide (19.7 x 11.8 in.). Run-on and run-off tabs were

N. U. AHMED and B. L. JARVIS are with CSIRO, Div. of Manufacturing Technology, Adelaide Laboratory, Woodville, Australia.

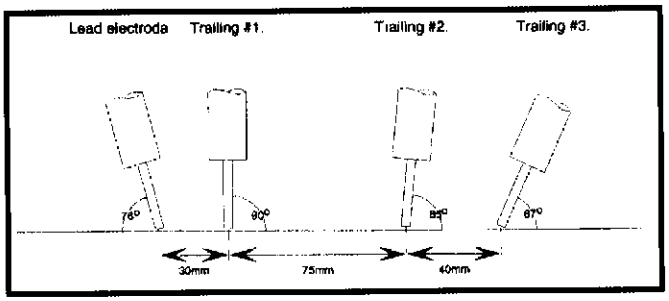

Fig. 1 — The electrode arrangement used during the study. Electrode extension was 30 mm.

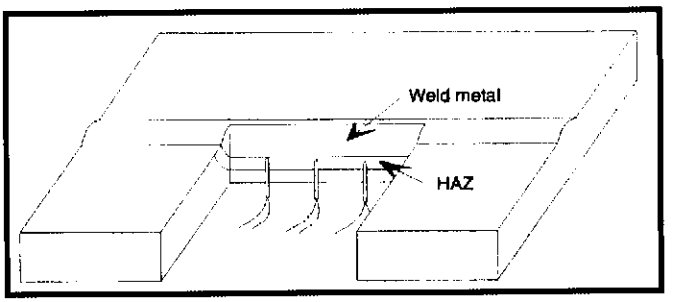

Fig. 2 — This diagram shows how the probes were placed for the measurements used in this study. The diagram is illustrative only, and not to scale.

added to allow the beads to extend over the entire length of the plate. The consumables used in the experiments were commercial 4-mm (0.16-in.) diameter electrode and a semibasic SAW flux suitable for the joining of such C-Mn steels. The chemical compositions are given in Table 1.

Welding Conditions

The welds were bead-on-plate made using a four-electrode process. The arrangement of electrodes is shown in Fig. 1. The polarity was DCEP, AC square, AC square and AC sine, for leading, first, second and third trailing electrodes, respectively. Electrode electrical extension was nominally 30 mm (1.2 in.), with allowance being made for the buildup due to metal deposition.

The welding conditions are detailed in Table 2. The decrease in the current-to-voltage ratio from the first to last electrode was necessary to achieve the required bead profiles. The heat input given was the calculated overall value, and an arc efficiency factor of one was assumed. It was apportioned almost equally between the arcs.

Thermocouple Preparation

The thermal cycles were obtained from thermocouples spanning the HAZ directly below the weld centerline, as shown in Fig. 2. The thermocouple depths were decided from cross-sections taken from preliminary welds made under the specified conditions. The depth of the fusion lines below the plate surface varied from about 3 to 15 mm (0.12–0.6 in.), and the HAZ widths at the weld roots varied from 1 to 4 mm (0.04–0.16 in.).

The plates were prepared by drilling a set of 15 holes of varying depth along and underneath the weld line. The holes were 1.8 mm (0.07 in.) in diameter, and spaced at 10-mm (0.4-in.) intervals. Once the holes had been thoroughly cleaned of swarf, oil and moisture, the probes were capacitively welded into position.

Each probe consisted of a pair of 0.35-mm (0.14-in.) diameter Pt-Pt 13% Rh thermocouple wires threaded through a short length of twin-bore, 1.6-mm (0.06-in.) diameter alumina sheathing. The wires were fused together at the tip before insertion.

Table 1 — Elements Other Than Iron in the Steel Plate and Filler Wire Metal, and the Chemical Composition of the Flux Used in This Study

	Analysis of plate and filler wire		Analysis of flux	
Element	% in plate	% in wire	Compound	% in Flux
C	0.24	0.13	SiO_2	16.3
S	0.16	0.014	TiO_2	0.09
P	0.032	0.012	Al_2O_3	17.8
Si	0.02	0.57	Fe_2O_3	0.65
Mn	0.83	1.25	MnO	1.43
Ni	0.016	0.02	MgO	27.2
Cr	0.016	0.05	CaO	26.1
Mo	<0.005	0.01	Na_2O	1.92
W	<0.005		K_2O	1.23
Cu	0.005		P_2O_5	0.04
Sn	<0.005			
Al	<0.005	<0.002	LOI	6.24
Ti	<0.005	0.05		
B	0.005	0.005		
Nb	<0.005	<0.01		
V	–	0.01		

Data Acquisition

The thermocouple signals were electrically isolated and amplified before being read into an IBM XT computer via a 16-channel, 12-bit analog-to-digital card. The acquisition software provided data conversion and storage to floppy disk. The outputs of all 15 probes and a temperature reference cell were recorded five times per second.

Weld Pool Ejection

To provide a visualization of weld pool shape as influenced by welding conditions, several weld pools were decanted. This was achieved by hinging the plate over the edge of the welding table and using an arrangement by which it could be rapidly swung back to a vertical position, impacting heavily with a stationary block in the process. The mechanism was spring loaded, and configured such that when triggered, the welding currents were simultaneously cut off. It took less than 0.2 s from release to impact. The liquid metal that was not ejected produced a skin over the crater floor, and since this was thin in comparison to the crater depths (*i.e.*, less than 5%), the results were considered to be adequate for their purpose.

Results and Discussion

Thermal Cycles

Presentation

The program of welding trials produced too much data for all to be presented. However, two complete sets of results are shown in Fig. 3 to illustrate the characteristics of the thermal cycles.

Each response was considered in two parts: a heating period consisting of several temperature excursions, and a concluding period of continuous cooling. The latter was specified by the time required to cool from 800° to 500°C

Table 2 — Welding Parameters Used During This Study

Plate (mm)	Heat Input (kJ/mm)	Speed (mm/min)	Electrode Current and Voltage (A, V)							
			Lead		Trailing 1		Trailing 2		Trailing 3	
20	2.5	1000	400	25	400	27	350	30	350	32
20	2.5	1500	550	25	500	30	500	35	500	38
20	2.5	2000	850	25	700	30	600	35	600	42
20	5	1000	900	25	700	30	600	32	600	35
20	5	1500	1050	32	900	35	750	40	650	46
20	5	2000	1300	30	1200	35	1100	40	950	45
20	10	600	950	28	800	32	700	35	600	40
20	10	1000	1200	35	1100	38	1000	40	1000	45
20	10	1300	1300	40	1200	40	1200	45	1200	45
50	2.5	1000	400	25	400	27	350	30	350	32
50	2.5	1500	650	25	550	28	480	32	450	35
50	2.5	2000	900	25	700	30	600	32	600	35
50	2.5	3000	1050	32	900	35	750	40	650	46
50	5	1000	900	25	700	30	600	32	600	35
50	5	1500	1050	32	900	35	750	40	650	46
50	5	2000	1300	30	1200	35	1100	40	950	45
50	10	500	900	25	700	30	600	32	600	35
50	10	1000	1300	30	1200	35	1100	40	950	45
50	10	1300	1350	41	1250	42	1200	45	1100	47

($\Delta t_{8/5}$)(1472° to 932°F), which is taken as the solid-state transformation time for steel. The heating period was more complex, but its essential features can be represented by the values of the temperature peaks and troughs, and the separations between them.

The direct comparison of thermal data from different welds was difficult because the thermocouples could not be positioned at a common point within the plate, or at an exact distance from the weld interface — Fig. 2. To overcome these difficulties, a representative signal, or signature, was determined by interpolation (see Appendix 1) from each set of data. This signature was defined as that response having a maximum temperature of 1350°C (2462°F). Some examples are given in Fig. 4. Each signature would have corresponded to a measurement taken just below the point of maximum fusion zone penetration. Measurements of probe positions made after welding indicated that the specified peak temperature would have been reached within 200 pm of the weld interface. Cooling times at this point should be approximately the minimum values within the HAZ for a particular weld. This temperature was chosen so that reliable responses at both higher and lower temperatures would be available for interpolation. Responses above 1450°C (2642°F) were generally unavailable or unreliable due to probe damage.

Interpretation of the Peaks

The heating phase of each thermal cycle contained between one and four peaks. Furthermore, those with less than four distinct peaks often exhibited regions of inflection, so that a common pattern was evident in all responses (Fig. 4 for example). This pattern, together with the $\Delta t_{8/5}$ values, provided the basis for the numerical values in Table 3.

The most likely explanation given for this pattern was that the succession of peaks resulted from the successive transits of the welding arcs. This was tested by comparing the spacing between peaks with the spacing between the electrodes. The results of these calculations are presented in Table 4. The close agreement between the mean observed positions and the calculated arc positions confirmed the arcs as the causes of the peaks.

Cooling Behavior

The $\Delta t_{8/5}$ values shown in Table 3 were found to increase with increasing heat input, and decrease for increased plate thickness. When welding speed was varied while heat input and plate thickness were kept constant (Table 3), the only significant change in $\Delta t_{8/5}$ was a substantial increase in value for welding speeds below 1000 mm/min (39 in./min). In other cases, the variations in

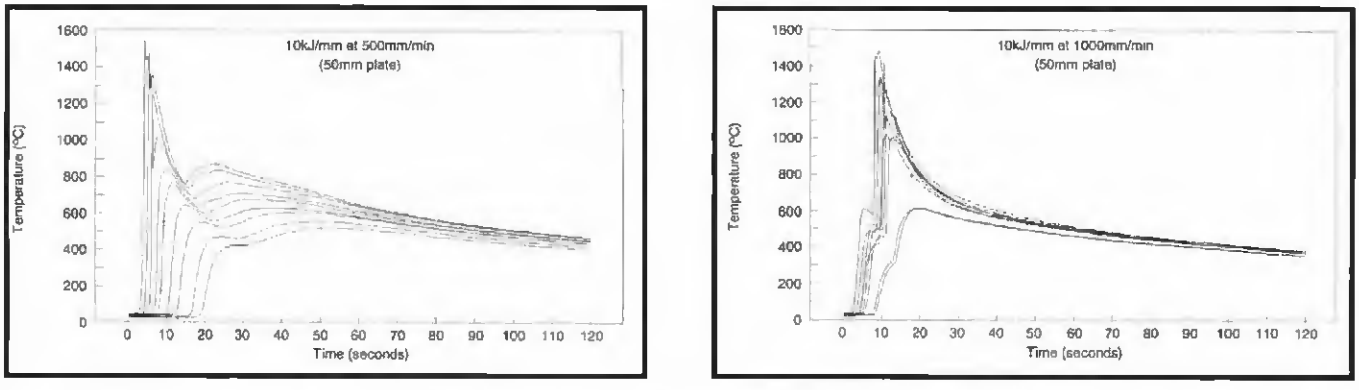

Fig. 3 — These plots show the thermal responses recorded at various depths below the weld roots in two separate trials. The trials were at the same heat input but different welding speeds. A — 500 mm/min; B — 1000 mm/min.

$\Delta t_{8/5}$ with welding speed were small, and appeared to be random.

An exception to the above comments was the 2.5 kJ/mm (63.5 kJ/in.) weld at 1500 mm/min (59 in./min) in 50-mm plate. This illustrates how the time a particular location spends in cooling between two temperatures can generate inconsistent results when several arcs are present. Figure 5 illustrates this particular situation in which the final temperature peak was 791°C (1456°F). In this case, the time spent between 800° and 500°C was extended by several seconds (17.3 s) because the beginning of the interval had to be associated with one of the preceding arcs. As a comparison, it took only 13.2 s to cool from 780° to 480°C (1436° to 896°F).

The retention times above 1100°C (2012°F) (RT-1100°C) were also determined for these trials, and the results are presented in Table 5. This measurement is important because both the extent of grain growth, and precipitate stability, are determined during this part of the thermal cycle (Ref. 6). The values varied with different welding conditions without any apparent pattern, even for constant heat input and plate thickness. The metallurgical significance of these variations is yet to be investigated.

The highest RT-1100 values were 13.1 and 18.0 s for the 10 kJ/mm (254 kJ/in.) welds on 20-mm plate. These were considerably longer than for any other weld, apparently due to the reduced thickness of the plate. Values for equivalent welds on 50-mm plate were close to 4 s.

In summary, the multi-arc thermal cycle consisted of overlapping responses to each arc, resulting in a succession of temperature peaks that could be separated by substantial amounts of cooling. This thermal behavior gives rise to difficulties both in definition and interpretation of conventional parameters such as $\Delta t_{8/5}$ and RT-1100°C, and so puts some doubt on their predictive power under these conditions. A more appropriate method of description is required, and

Table 3 — Thermal Cycles Representing Each Choice of Welding Conditions

Heat Input kJ/mm	Speed mm/min	Temperature in °C Peak 1	Min 1	Peak 2	Min 2	Peak 3	Min 3	Peak 4	$At_{8/5}$ s
				20 mm plates					
2.5	1000	1195	1004	1350	859	954	1011	1130	17.0
2.5	1500	562	609	1350	802	897	917	1135	14.8
2.5	2000	938	777	1140	854	1350	1219	1315	18.0
5.0	1000	1350	926	1331	804	961	990	1045	61.2
5.0	1500	192	261	754	613	1350	1250	1236	68.7
5.0	2000			374	498	1350	1048	1060	57.6
10.0	600	1008	1054	1350	948	1217	1188	1192	241.2
10.0	1000			886	765	1350	1321	1331	183.2
				50 mm plates					
2.5	1000	673	703	1350	837	891	906	1026	9.8
2.5	1500	1350	833	884	727	760	758	791	17.3
2.5	2000	1265	1041	1350	832	989	912	915	11.3
2.5	3000	909	752	1350	1093	1067	970	970	9.2
5.0	1000	1284	1121	1350	809	825	809	828	23.8
5.0	1500	618	661	1350	856	1104	992	983	23.8
5.0	2000			510	518	1350	1168	1207	18.2
10.0	500	1350			726	802	812	827	73.8
10.0	1000			507	499	1350	1187	1174	42.0
10.0	1300			300	412	1260	1281	1350	42.0

Note: In some cases the values of the peaks or troughs could only be determined from the second derivative. This can result in a peak with a lower value than an adjacent trough, as has occurred in a few instances.

Table 4 — Least Squares Fit of the Calculated Peak Positions to the Electrode Spacings[a]

Heat Input kJ/mm	Speed mm/min	Position in mm Peak 1	Min 1	Peak 2	Min 2	Peak 3	Min 3	Peak 4
				20 mm plates				
2.5	1000	−3	21	31	94	111	128	141
2.5	1500	11	26	31	91	101	106	136
2.5	2000	7	24	38	91	104	118	131
5.0	1000	9	23	32	89	106	112	133
5.0	1500	14	21	44	89	104	111	119
5.0	2000			36	89	109	122	135
10.0	600	11	19	27	91	107	129	135
10.0	1000			36	76	116	122	129
				50 mm plates				
2.5	1000	7	17	27	91	104	117	141
2.5	1500	−2	17	27	78	103	123	153
2.5	2000	12	25	32	78	98	132	138
2.5	3000	−7	12	32	103	112	132	143
5.0	1000	4	11	24	91	104	138	148
5.0	1500	1	11	16	91	106	141	156
5.0	2000			56	69	89	116	136
10.0	500	−8			80	112	127	147
10.0	1000			49	76	92	132	139
10.0	1300			49	92	109	118	122
Mean position		4	19	35	87	105	124	138
Arc position		0		30		105		145

(a) Refer to Fig. 1. The mean positions are also shown.

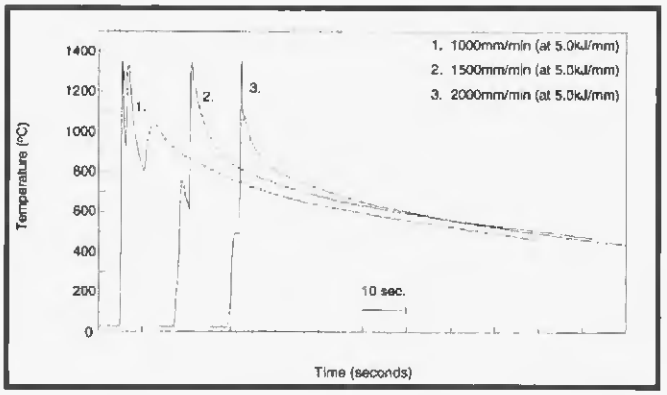

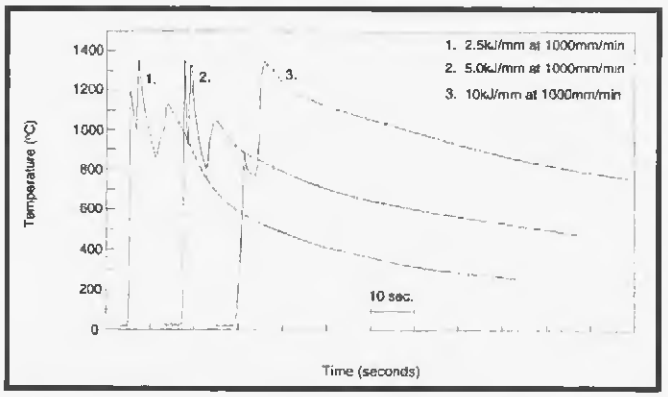

Fig. 4 — These responses show the effect of varying welding speed. A — at fixed heat input; B — varying heat input at constant welding speed. The welds were made on 20-mm plate.

this may need to consider the temperature dependence of the various metallurgical changes taking place.

The Effect of Welding Parameters on the Thermal Cycles

Variation of Welding Speed and Heat Input

Plots, such as in Fig. 4A, show that the signatures of welds of the same heat input differed significantly at different welding speeds. These differences occurred during the heating period, and related to the amplitudes of the peaks and the times separating them. The details of changes in peak amplitudes often appeared random, as seen from Table 3. However, as speed increased, the separate peaks became more difficult to resolve, and the signatures approached that of a single heat source (*i.e.*, consisting of a single peak). This trend has also been noted previously (Ref. 6). In addition, the signatures for trials at constant welding speeds varied with heat input — Figs. 3, 4B. In these cases, the differences related to both the amplitudes of the peaks and the cooling times. The signatures tended toward that of a single heat source as heat input increased.

Several trials were conducted where the currents and voltages applied to each arc were kept constant, while both welding speed and heat input were allowed to vary — Table 2. Under these conditions, the relative amplitudes of the peaks remained approximately constant, while the time separating them and the resultant cooling time both varied. These features are evident in Fig. 6A and 6B, respectively.

Arc Parameters and Peak Temperature

The fact that the highest peak in the thermal signature usually did not coincide with the location of the final arc indicated that the thermal cycle was dependent on the individual arc parameters, as well as total heat input. The effects of these parameters, notably current and voltage, have not been satisfactorily treated and quantified theoretically, although they are recognized in practice.

It is standard practice that the first pair of electrodes should be used to obtain joint penetration, and the last for control of bead shape. Penetration of a single arc increases with current for a given heat input and welding speed, and decreases as the angle between the electrode and the normal to the plate increases. These relationships were used in an attempt to achieve satisfactory results. In seven out of the ten 50-mm plates, the peak temperature was associated with either the first or second arc (Table 3) consistent with the desired penetration behavior. In fact, in three cases the higher peak for the second pair of arcs was over 500° below the 1350°C peak, and the associated temperature rise was under about 100°C (180°F). This is consistent with a reduction in penetration between the leading and trailing pairs of arcs. Thus the characteristics (such as penetrating power) of an arc in a single electrode environment may serve as a first approximation for its behavior in a multi-electrode application, despite the presumed formation of a single, continuous weld pool. However, cumulative effects are also important and must be considered when explaining the final results. This is exemplified by the three above-mentioned responses where the temperature peaked during the passage of the trailing pair of electrodes, which is not explicable in terms of single arc behavior alone.

Plate Thickness

The influence of plate thickness on cooling times has been extensively studied by many researchers, including Rosenthal (Refs. 8, 9) and Easterling (Ref. 6). They predicted a lengthening of cooling time as the heat flow changed from three-dimensional (*i.e.*, thick plate) to two-dimensional (thin plate). This effect was quite noticeable in this study, as indicated by the $\Delta t_{8/5}$ values in Table 3.

Plate thickness may be taken into account by considering the plate boundaries as heat reflectors (a standard mathematical technique) (Refs. 9, 10). Since in multi-electrode welding the time taken for all the electrodes to pass a particular point may be ten or more seconds, these

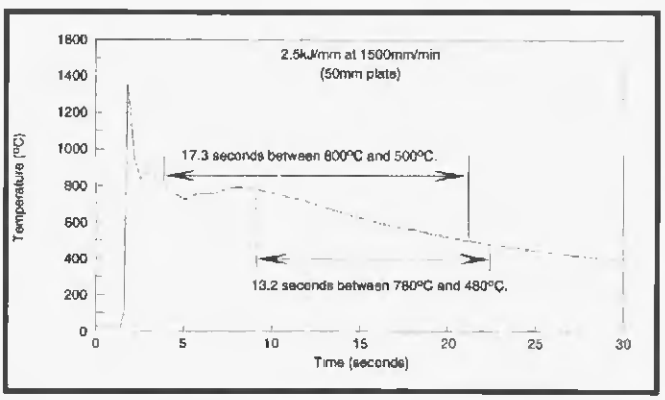

Fig. 5 — This figure demonstrates the difficulties that can arise if the cooling behavior is described in terms of the time required to pass between two limits.

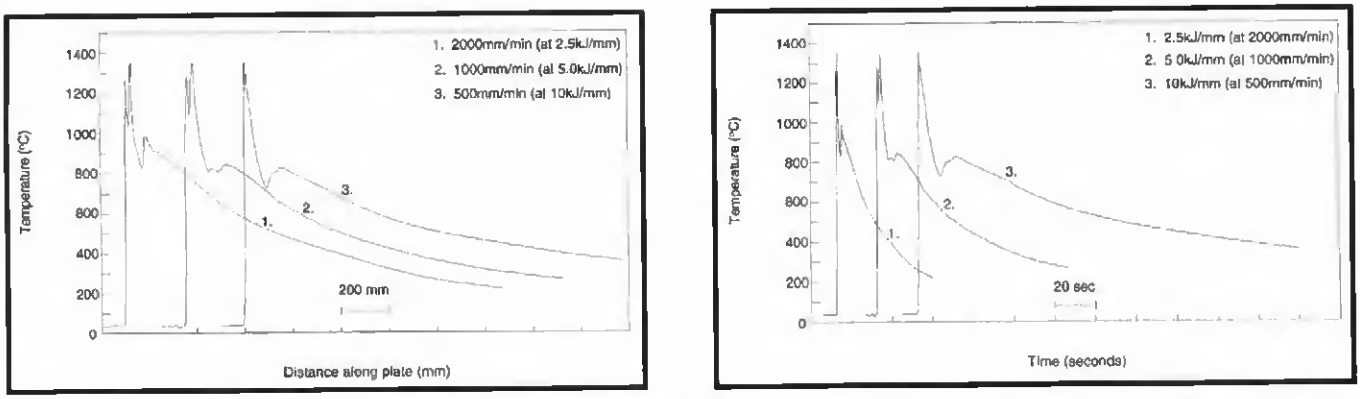

Fig. 6 — Signature from welds with the same current and voltage conditions, but differing welding speeds. A — plotted against distance; B — plotted against time. The welds were made on 50-mm plate.

reflections may become significant before the heating period has been completed.

An example of the effect of plate thickness on thermal cycle observed is shown in Fig. 7. In this case heat input, welding speed and welding parameters for each electrode were constant and only the plate thickness was altered. In general, the traces show that the thermal cycles were more dependent on plate thickness when current density was high (deep penetration) or welding speed was low.

Relationships between the Thermal Response and Weld Pool Geometry

Determinations of the Fusion Boundary

The thermocouple data were consistent with a weld interface that varied, but did not necessarily increase, in depth from the first to last electrode. In order to gain some further insight into the relationships between the arcs and the thermal effects, the geometry of the weld pools was examined.

Two approaches were available. The first of these involved the extraction of cross-sections of completed welds. Four examples, representing approximately the extremes in the observed profile geometries, are presented in Fig. 8. The first two (8A and 8B) contain several weld interfaces of differing joint penetration. For each case it can be argued that the line corresponding to the least penetration was necessarily the last formed, because it would have been destroyed had there been a subsequent increase in pool depth. Therefore, in these two examples, the penetration of the last arc was considerably less than the maximum. This confirms the hypothesis presented earlier that in some cases the weld pool was deeper below the leading pair of electrodes than below the trailing pair. On the other hand, for Fig. 8C and 8D, the joint penetration of the last arc was approximately equal to the maximum. These observations are consistent with the corresponding thermal cycles as summarized in Table 3.

Thermal Cycles away from the Root of the Weld

A cast replica of one of the craters left after weld pool ejection is shown in full, and in longitudinal section, in Fig. 9A and B. It shows the thermal history of the weld as a single isothermal surface. This is made clearer in Fig. 10 where successive cross-sections show how the bead profile and HAZ developed as the weld progressed.

Since the voltage always increased from first to last electrode, and the bead width increased with voltage, the width was finally established by the last arc. It follows that, if the last arc also determined the maximum penetration of the weld bead, then it determined the entire boundary. However, if the maximum depth was produced earlier in the weld cycle, then different boundary elements must have been established at different times — Fig. 8A to D. Thus, for welds with single weld interfaces, all points on the fusion boundary reached their peak temperatures simultaneously. They would therefore have experienced similar cooling behavior. This is reflected in the relative uniformity in HAZ width, as evident in Fig. 8C and D. On the other hand, weld interfaces as in Figs. 8A, 8B and 10, were made progressively. The temperatures under the roots of these welds peaked with the second arc, and were less affected by the third and fourth arcs. In the near-surface HAZ the peaks would have been after the last arc, with possibly little effect from those preceding it. Finally, the area near the intersection of the boundary segments could be predicted to have been strongly heated by all the arcs, resulting in a long retention time at a high temperature. This was supported by the observation of very coarse grains and wide HAZ of that region — Fig. 11.

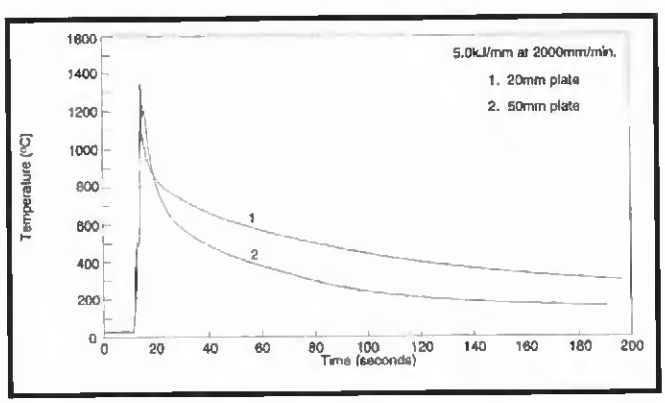

Fig. 7 — These plots demonstrate the effects of plate thickness on cooling behavior. A — 5 kJ/mm at 1000 mm/min; B — 10 kJ/mm at 500 mm/min; C — 5 kJ/mm at 2000 mm/min; D — 10 kJ/mm at 1000 mm/min.

Applications of Solidification Front Data

Examination of the weld pool geometry in multi-electrode welding is a powerful tool for determining the effects of each arc and understanding the thermal responses. Although cross-sections of completed welds are useful, it is believed that the three-dimensional view provided by weld pool ejection is more informative. Not only has this approach shown that joint penetration may either increase or decrease with successive electrodes, but it provides a simple method of quantifying this behavior. It is

also of practical significance that by exposing the solidification front, the effects of each arc is revealed in a visible and readily interpreted manner.

The determination of the solidification front has potential applications in two other areas. Since it presents a surface of known temperature, it should be possible to use it to obtain quantitative data on the thermal cycle at any point of the plate, including within the solidified weld metal. In particular, the surface would supply the boundary condition necessary for solving the heat flow equations in the weldment. The advantage of this approach is that it bypasses the need to model the weld pool itself, bringing it well within the capabilities of available software. On a more practical level, the method may well prove useful in the development of multi-arc welding procedures. This work has shown that the shape of the solidification front and the thermal cycle are linked, and dependent on the chosen welding conditions. However, measurements of the thermal cycles are difficult and very time consuming. Consequently, by gaining rapid access to the solidification front geometry, the welding engineer will be in a better position to determine the most appropriate welding conditions for any application. It is suggested that both areas merit further investigation.

Conclusions

For the conditions investigated, the following conclusions can be drawn:

1) The thermal responses consisted of a series of temperature peaks, which correlated with individual arcs, followed by a continuous cooling phase. The main factors influencing the shape of the thermal response were the individual arc current and voltage settings, and welding speed. Consequently, welds at different welding speeds but the same heat input gave quite differently shaped responses.

2) There was an increase in $\Delta t_{8/5}$ for the 10 kJ/mm welds with welding speeds below 1000 mm/min. At other heat inputs, however, $\Delta t_{8/5}$ values did not show any definite trend with welding speed, although welding speeds remained above 1000 mm/min. The cooling times were drastically affected by changing heat input through variation of either welding speed or arc current and voltage values.

3) The variation in the retention times (RT-1100°C) at constant heat inputs but different welding conditions were large and appeared random.

4) Conventional indicators such as RT-1100°C and $\Delta t_{8/5}$ must be used with caution when dealing with multi-electrode welding. New measurements that allow for the complex thermal behavior generated by this process need to be devised.

5) Increasing either the welding speed at constant heat input or the heat input at constant speed in multi-electrode welding caused the thermal response to approach that of a single electrode.

6) Reducing plate thickness from 50 to 20 mm resulted in a large increase in cooling times. The reduced heat dissipation capability increased the preheating effects of the first and second arcs, thus enhancing the joint penetration of the trailing arcs. These influences became more pronounced with increasing heat input and decreasing welding speed.

7) The width and depth of the weld pool varied nonuniformly along its length, and changes to the welding parameters caused the point of maximum penetration to be associated with differing electrodes.

8) Weld pool ejection provided a sim-

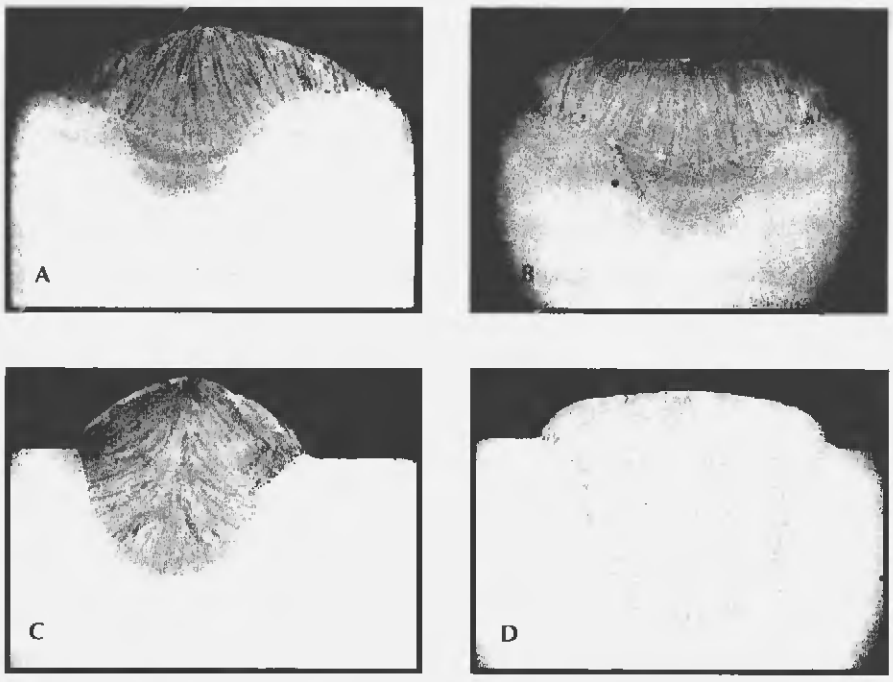

Fig. 8 — This selection of cross-sections shows some of the variation in profile that occurs as the welding conditions are changed. All the above cross-sections were taken from 50-mm plates. A — 5 kJ/mm at 1000 mm/min; B — 10 kJ/mm at 500 mm/min; C — 5 kJ/mm at 2000 mm/min; D — 10 kJ/mm at 1000 mm/min.

Table 5 — Variability in the Relation Times above 1100°C

Heat Input (kJ/mm)	Speed (mm/min)	RT-1100°C (seconds) 1st interval	2nd interval	3rd interval	Total Time
		20 mm plate			
2.5	1000	0.6	1.5	1.2	3.3
2.5	1500	0.4	0.7		1.1
2.5	2000	0.4	2.3		2.7
5.0	1000	0.3	1.1		1.4
5.0	1500	2.2			2.2
5.0	2000	0.4			0.4
10.0	600	2.8	10.3		13.1
10.0	1000	18.0			18.0
		50 mm plate			
2.5	1000	1.0			1.0
2.5	1500	0.3			0.3
2.5	2000	0.2	0.2		0.4
2.5	3000	1.7			1.7
5.0	1000	0.7	1.8		2.5
5.0	1500	0.8	0.2		1.0
5.0	2000	2.2			2.2
10.0	500	3.3			3.3
10.0	1000	4.8			4.8
10.0	1300	3.3			3.3

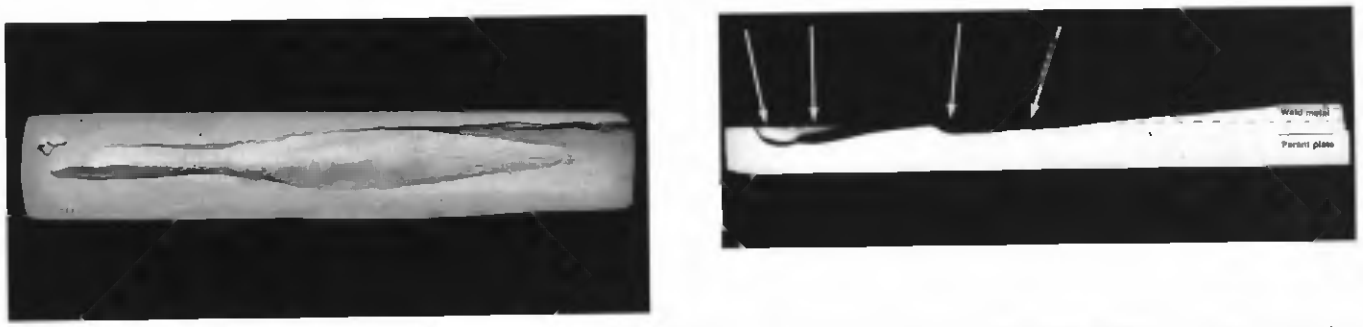

Fig. 9 — View of the replica of the crater. A — longitudinal section; B — 10 kJ/mm at 500 mm/min on 50-mm plate. The arrows indicate the electrode positions when the pool was decanted.

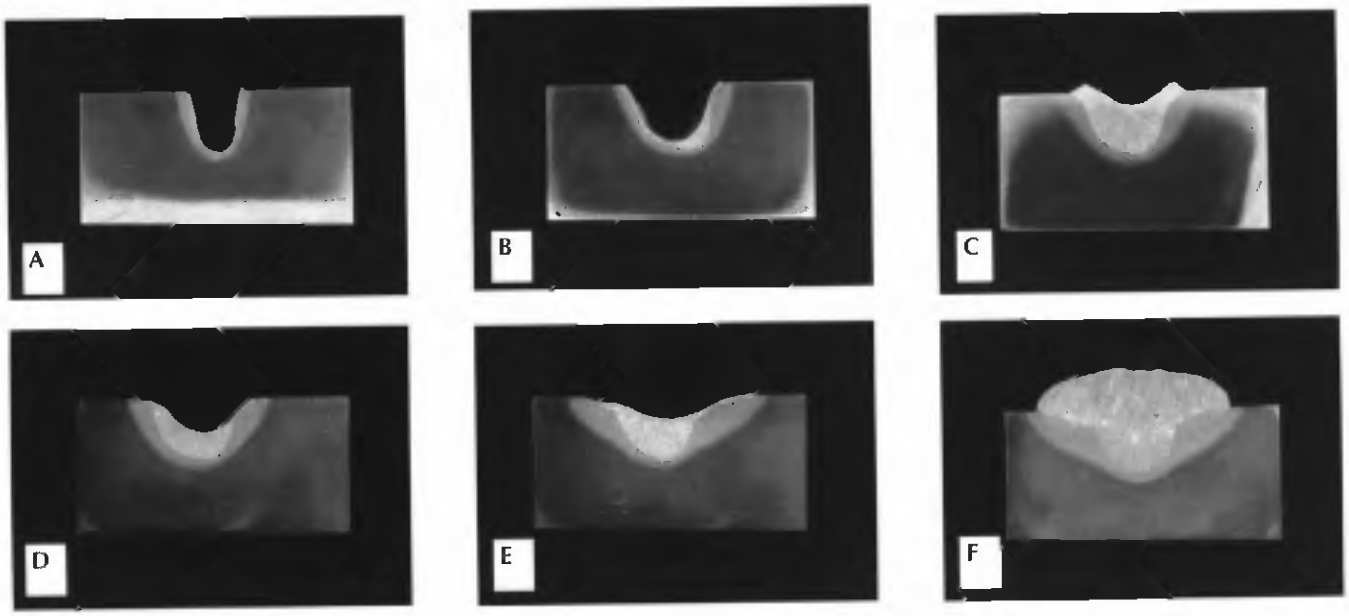

Fig. 10 — Cross-sections from a weld that was interrupted and rapidly decanted. The weld was made at 10 kJ/mm and 500 mm/min on 50-mm plate. A — First electrode; B — second electrode; C — between second and third electrodes; D — third electrode; E — fourth electrode; F — final profile.

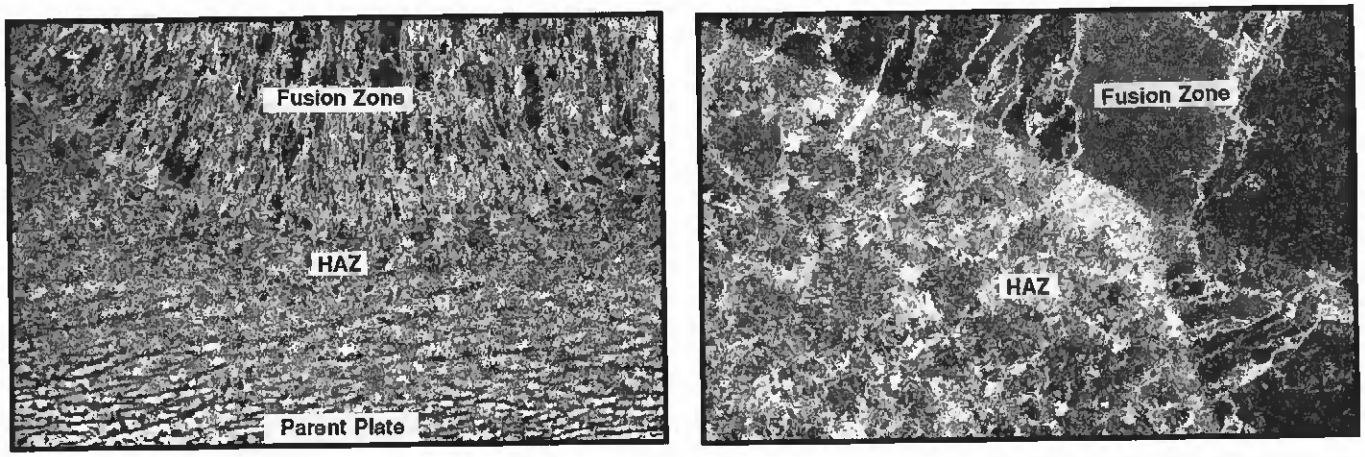

Fig. 11 — Micrographs of welds shown in Fig. 10 (10 kJ/mm, 500 mm/min; 50-mm plate). A — Below the root; B — near the intersection of the second and last weld interfaces. Magnification, 25X.

ple method of studying the weld pool boundaries in multi-electrode welding. It may offer a visual means for use in tailoring the weld pool shape and resultant thermal cycles generated in the base material.

References

1. Knight, D. E. 1954. Multiple electrode welding by the "Unionmelt" process. *Welding Journal* 33(4): 303–312.

2. Taylor, D. S., and Thornton, C. E. 1989. High deposition rate submerged arc welding. *Welding Review* 8(3): 167–180.

3. Bhadeshia, H. K. D. 1990. Control of weld microstructure and properties. *Proc. of Int. Conf. on the Metallurgy of Welding, and Qualification of Microalloyed (HSLA) Steel Weldments*, Houston, Tex., p. 726.

4. Nomura, H., Sugitani, Y., and Nakagawa, H. 1989. Magnetic force in multi-electrode submerged arc welding. *Proc. Arc Physics and Weld Pool Behavior*, pp. 311–323.

5. Kitamura, Y., Fujimori, S., and Yatake, T. 1988. Dynamic observation of a molten pool in submerged arc welding with high travel speed. *IIW Asian Pacific Regional Welding Congress*.

6. Easterling, K. 1983. *Introduction to the Physical Metallurgy of Welding*. Published by Butterworths, London.

7. Painter, M. J., and Jarvis, B. L. 1992. Numerical modeling of the submerged arc welding process. *Modeling and Control of Materials Processing Conference*. Wollongong, Australia.

8. Rosenthal, D. 1941. Mathematical theory of heat distribution during welding and cutting. *Welding Journal* 20(5): 220-s to 234-s.

9. Rosenthal, D. The theory of moving sources of heat and its application to metal treatments. *ASME Transactions*, Vol. 68, pp. 849–866.

10. Boas, M. L. 1966. *Mathematical Methods in the Physical Sciences*. Published by Wiley and Sons, Inc.

Appendix

The comparison of thermal responses obtained under different welding conditions requires that they should have achieved the same peak temperature. Experimentally, this was impossible due to the uncertainty in weld pool behavior and probe positioning. Consequently, the responses used in this work were obtained by interpolation.

Each thermocouple response consisted of a set of 1000 temperature readings spanning the weld cycle, and taken at 0.2-s intervals. For each set of responses, the two closest to, but on either side of, a 1350°C peak temperature were selected (T1 and T2).

Since the responses were sharply peaked, the logarithms of the readings (ln(T1) and ln(T2)) were taken. The two sets of numbers (ln(T1) and ln(T2)) were then aligned by offsetting the time base of one with respect to the other to maximize the correlation between them. This was determined numerically.

At this stage the logarithm of a new response (T3) could be obtained by linear interpolation:

$$\ln(T3) = \ln(T1) + k \cdot (\ln(T2) - \ln(T1))$$

where k is an arbitrary constant. The actual response is the exponential of this:

$$T3 = \exp(\ln(T1) + k \cdot (\ln(T2) - \ln(T1)))$$

The value of k was obtained by numerically solving for the desired peak temperature of T3 for each pair of T1 - T2 values.